Solar Energy 239 (2022) 242–251

Contents lists available at ScienceDirect

Solar Energy

journal homepage: www.elsevier.com/locate/solener

# The performance and amphibious operation potential of a new floating photovoltaic technology

Torunn Kjeldstad [a], Vilde S. Nysted [a,*], Manish Kumar [a], Sara Oliveira-Pinto [b], Gaute Otnes [a], Dag Lindholm [a], Josefine Selj [a]

[a] Institute for Energy Technology, Instituttveien 18, 2007 Kjeller, Norway
[b] Equinor ASA, Forusbeen 50, 4035 Stavanger, Norway

ARTICLE INFO

*Keywords:*
Floating PV
U-value
Module temperature
Performance
Amphibious operation

ABSTRACT

Floating photovoltaics (FPV) is a rapidly emerging technology that provides an alternative to ground-mounted PV (GPV), particularly where land is scarce or expensive. Despite an impressive technological development and growth in installed capacity in recent years, studies on the performance and reliability of FPV are scarce. This work provides insight with respect to the performance, reliability, and operational characteristics of a new FPV technology with the aim to identify innovation opportunities, reduce risks, develop improved solutions, and improve bankability of FPV. We have analysed production and weather data from one year of operation for an open FPV system with a small water footprint located on a water body in Kilinochchi, Sri Lanka. The technology is developed by the company Current Solar. Using established filtering routines and algorithms from pvlib, the yield and performance ratio is calculated and compared to a GPV system installed on the shore of the lake. We find that the technology gives a stable overall performance over the one-year period, and that the period of amphibious operation did not impact the continued performance of the system. Calculations of the U-value of the system, based on the production and weather data, gives a median U-value of 33 $W/m^2K$, slightly higher than the default PVsyst value of 29 $W/m^2K$ for freestanding GPV systems. The calculated U-values are used in an energy yield analysis in PVsyst to estimate the energy production of the FPV technology and benchmark it against measured data.

## 1. Introduction

### 1.1. FPV market and research challenges

Worldwide demand for energy is continuously rising. Concurrently, there is an urgent need to reduce greenhouse gas emissions to avoid further irreversible warming with profound economic and humanitarian consequences (IRENA, 2021). Hence, it is paramount to decouple energy use from its current emissions and renewable energy is one of the key pillars of the energy transition (IRENA, 2021).

The renewable energy sector currently experiences an unprecedented growth, with decreasing costs, rising investments, and technology innovation. In 2020, renewable energy increased by 3% while demand for all other energy sources, particularly oil and coal, declined due to Covid19 (IEA, 2021). Photovoltaics (PV) is the renewable energy with the greatest growth in the past decade and in many markets solar is now cheaper than any power source ever before (IEA, 2020). However, in certain areas, PV deployment will be limited by lack of available land resources and competition for land usage. Floating PV (FPV) has emerged as a solution that will allow untapped surfaces to be turned into viable and value-adding commercial solar installations, avoiding conflicts with agricultural or residential uses (Cagle et al., 2020; Gadzanku et al., 2021).

The FPV marked is experiencing a rapid growth reaching a cumulative rated installed capacity of >3GW by the end of 2021 (Paton, 2021), with most of the FPV projects installed in Asia, followed by Europe. For instance, the Netherlands aims to have a cumulative rated installed capacity of ~2GW by 2023 (Folkerts et al., 2017). Globally, FPV is expected to grow by an average of 22 % year-over-year through 2024 (Cox, 2019). The technology landscape is mainly targeting FPV applications in enclosed freshwater bodies, such as lakes, but there is already a focus from the sector to search for opportunities among marine applications (Oliveira-Pinto and Stokkermans, 2020).

Even as the capacity of FPV systems is increasing rapidly, there are

* Corresponding author.
*E-mail address:* vilde.nysted@ife.no (V.S. Nysted).

https://doi.org/10.1016/j.solener.2022.04.065
Received 28 February 2022; Received in revised form 12 April 2022; Accepted 30 April 2022
Available online 17 May 2022

still challenges related to performance and reliability that needs to be solved. This is mostly due to the lack of accessible, long-term production and monitoring data from FPV systems. The published analysis and literature are gradually increasing, but with the range of different climates, technologies, and relevant parameters the need for more data to improve the bankability, and reliability, of FPV is substantial.

The aim of this work is to provide insight into the performance, reliability, and operational characteristics of a new FPV technology. The following Section, 1.2, will provide a short review of the literature on performance and reliability of FPV technologies in general. Several operational characteristics that impact the performance, differ between ground-mounted PV (GPV) and FPV. This includes mismatch losses, soiling losses and efficiency of heat transfer from the modules. In this work we explicitly study the efficiency of the heat transfer for the Current Solar FPV technology, and Section 1.3 provide background on this topic.

### 1.2. Performance and reliability of FPV

The literature in the field of FPV performance is gradually increasing, and DNV GL recently published the first guidelines for energy yield assessments (EYA) of FPV (DNV GL, 2021). The performance and reliability of the FPV systems depends on various factors such as system mounting structure, PV technology, orientation, local environmental parameters, cooling mechanisms etc. The mounting structure and floating platform play an essential role in determining the performance of a PV system as it must bear the load of the module and environmental stresses (Kumar et al., 2021b). In addition, the floating structure can affect the cooling mechanism of the FPV system because of the direct and indirect contact of the module with the water and the exposure of the module to the surface area of the water. As a result, there is an impact on the performance of the FPV system (Cazzaniga et al., 2018). Rosa-Clot et al. (2010) compared air-exposed PV modules to submerged floating PV modules and found that the efficiency of submerged modules was increased by 20% compared to air-exposed modules. But such systems have challenges with respect to their long-term reliability. However, new developments are taking place due to the trade-off between the design, reliability and cost of floating structures. Earlier studies show variation in thermal loss coefficient of FPV modules as it is mainly dependent on installation design, floating PV structure, and PV technology. This results in variation in the performance of FPV systems.

All water bodies experience variations in water levels through the year, and for inland water bodies, larger fluctuations are to be expected throughout the lifetime of a FPV system. In particular, when placed on smaller water bodies, as is the case for the studied system, or those operated close to shore, there may be a need for amphibious operation, meaning FPV systems that can sustain reliable and stable operation also when they are exposed to water level fluctuations that leaves the FPV system sitting on dry land. This may also be relevant for installation of FPV on new hydropower dams. As FPV has substantially shorter construction time than hydropower dams, and it can be beneficial to be able to start the operation of the FPV system before the dam has been constructed. Amphibious operation poses challenges such as the need for a flexible mooring that can handle varying water levels and sufficient anchoring of the system on dry land. Also, the curvature of the seabed can change the POA of the individual modules when the system is standing on the dry seabed. To our knowledge, there has been no reports on how amphibious operation affects the performance of FPV.

Losses in floating PV systems may be slightly different from land-based systems. In FPV, there is no loss of shading due to nearby objects and there is less dirt, but soiling loss from bird droppings can be prominent. Also, temperature inhomogeneity and misalignment in module orientation can potentially lead to mismatch losses (Gorjian et al., 2021). Besides these, the degradation of PV modules under the environment of water bodies is a matter of concern for the long-term reliability of PV modules. Modules are constantly exposed to humid environments which can accelerate various degradation modes such as bus bar corrosion, moisture ingression, leakage current and junction failure (Kumar et al., 2021a). Research on performance loss rates and reliability of FPV systems is still very limited, as solid analysis of reliability requires a time-series of several years. Thus, there is a need for long-term performance and degradation studies of floating PV systems with different technologies to identify these aspects.

A frequently stated advantage of FPV over GPV is the potentially reduced module temperature due to water cooling, resulting in a higher power conversion efficiency. While many claims have been made regarding enhanced cooling of FPV (Choi, 2014; Lee et al., 2014; Suh et al., 2020; Yadav et al., 2017 Do Sacramento et al., 2015; Ho et al., 2016; Majid et al., 2014), they have only to a limited extent been followed up by conclusive data or quantification and the significance of FPV technology has often been under-communicated in reviews and reports (Kjeldstad et al., 2021). However, several recent results and publications indicate that the cooling effect on the typical pontoon-based floaters is in fact modest (Liu et al., 2017, 2018; Mittal et al., 2017; Oliveira-Pinto and Stokkermans, 2020). Some studies have even reported a lower module performance on the water compared to land (Kumar et al., 2021a). A clear understanding and quantification of the cooling effect for the different FPV floater technologies is hence an important missing piece of information in the industry (Kumar et al., 2021b). It is essential to successfully optimize cooling against other performance and O&M-relevant aspects such as panel tilt, soiling and cleaning, panel mounting and robustness. This understanding is also needed for accurately estimating power production. Large uncertainties in predictions of cooling-enhanced performance directly converts into uncertainties EYA and levelized cost of electricity (LCOE) calculations.

The recently published best practice guidelines from DNV GL states that it is “recommended to apply different thermal loss factors for different types of systems and different float technologies”. However, in the absence of appropriate simulation software and technology specific recommended thermal loss factors, the current “best practice procedure is to determine the thermal loss factors for FPV systems through application of technology-specific measurements” (DNV GL, 2021). To diversify the available data in terms of technology and climatic characteristics and address the unanswered questions related to performance and cooling of various FPV technologies, it is of great importance to collect and analyse field data from a range of systems. This should preferably be accompanied with theoretical modelling to establish the weather dependency of the heat loss coefficients for different FPV technologies.

### 1.3. Module temperature and heat transfer coefficients

The operating temperature of a PV module is determined by several factors: incident solar radiation, ambient temperature, wind speed, wind direction, properties of the cell and module materials and mounting structure. Both radiative and convective heat transfer will take place and affect the module temperature. Numerous models have been proposed for simulation of the module temperature. A comprehensive overview is given by Skoplaki and Palyvos (2009) for GPV systems, the values of the heat loss coefficients and their correlation with various meteorological parameters has been thoroughly studied. In IEC61853-2 (IEC, 2018) the Faiman model is recommended as the preferred method to estimate the module temperature (K) in yield assessment analysis. In the model proposed by Faiman (2008) the electrical efficiency, η, is taken into consideration so that the fraction of the incident irradiance being converted to electrical energy is not considered to be contributing to the increase in module temperature, while this is not included in the standard. When the electrical efficiency is taken into consideration the module temperature, $T_{mod}$ (K), is given by.

$$T_{mod} = T_{amb} + \frac{G(\alpha - \eta)}{U_0 + U_1 v}, \quad (1)$$

where $T_{amb}$ (K) is the ambient temperature, α is the absorbed fraction of the incident irradiance, set to 0.9, G (W/m$^2$) is the incident irradiance and η is the electrical efficiency of the module. The heat loss coefficient of the system, $U_0 + U_1 v$, consists of a constant value and a wind component. If the wind component is not available, or the meteorological data lacks reliable wind measurements, a single value for the heat loss coefficient, U (W/m$^2$K), is often used and referred to as the U-value. Eq. (1) is also utilized in the industry standard modelling software for PV plants, PVsyst®. For GPV systems, the values of the heat loss coefficients and their correlation with various meteorological parameters has been thoroughly studied (Barykina and Hammer, 2017; Ghabuzyan et al., 2021; Koehl et al., 2011), but the most appropriate values of $U_0$ and $U_1$ for the various types of mounting structures are still debated. This is not surprising as the heat transfer will depend on module characteristics, outdoor conditions and mounting, and hence a significant spread in best fit values for different systems is expected. Even for identical modules installed at different sites with the same type of mounting, the best fit values for $U_0$ and $U_1$ was found in one study to have a spread of 14% in $U_0$ and 29% in $U_1$ (Barykina and Hammer, 2017). The weather conditions at a given site influence the parameters, as $U_1$ depends on the number of days with high irradiance (>400 W/m$^2$) and the corresponding range of the irradiance values, the amount of wind, and ambient temperature ranges on the chosen days. Naturally, these combinations of outdoor conditions are different for each of the sites. For many commercial energy yield assessments, also for utility scale PV plants, only a single U-value is used as input and no wind data is included.

Only a few studies report heat transfer coefficients for FPV systems directly (Dörenkämper et al., 2021; Liu et al., 2018). Many earlier studies infer the temperature differences by comparing the performance of GPV and FPV systems, often based on systems with limited monitoring (Choi, 2014; Kamuyu et al., 2018; Lee et al., 2014; Suh et al., 2020; Yadav et al., 2017). Other studies report on prototype FPV technologies that are in direct contact with water and where the water temperature therefore is expected to impact the module temperature to a greater extent than in commercially available systems (do Sacramento et al., 2015; Ho et al., 2016; Majid et al., 2014). Other studies that have found superior performance due to water cooling have utilized water as a cooling agent by either submerging the panels in water or spraying the panels with water. Various technologies exploiting this are detailed in the reviews by Cazzaniga et al. (2018) and Dwivedi et al. (2020).

More recent studies analysing production and monitoring data from fit for purpose instrumented FPV systems show that the additional cooling effect is highly FPV technology dependent (Dörenkämper et al., 2021; Liu et al., 2018). A thorough study of the performance of FPV systems in the Tengeh Reservoir testbed in Singapore show that while the FPV systems generally outperform the average Singaporean rooftop system, a well-ventilated roof-top system on shore performs slightly better than all the tested FPV systems (Liu et al., 2018). The observed lower operating temperature for some FPV systems (excluding those that have active cooling or are lying on, or in, the water) compared to GPV systems is predominantly due to local climate differences. Large water bodies will often provide lower ambient air temperatures and higher windspeeds than dry land. A literature review (Völker et al., 2013) found that during daytime and in the summer the cooling effect of ponds, lakes, and rivers is between 0.5 and 5 K, and the range of this effect is between a few meters and up to 400 m. For larger water areas, maximum wind speed increases and the effect of the water body is detectible at greater distances. Even around a small pond of 0.25 ha significant wind speeds can develop, but only at short distances (Gross, 2017). Amiot et al. (2020) found that the theoretical offshore wind was roughly twice the onshore wind for a small pond with a perimeter of 1,05 km. For low wind speeds, radiative cooling will have a relatively more important role and the temperature of the surfaces that is seen by the module will then have a small effect on the temperature of the module (Lindholm et al., 2021). Naturally, the effect of all these parameters will depend heavily on the mounting structure of the FPV system.

### 1.4. Objectives

This study reports on the performance of a small footprint FPV system developed by the company Current Solar. The pilot is located on a freshwater body in Kilinochchi, Sri Lanka and has been operated since January 2020. A GPV system is installed on the shore of the same water body, and near the FPV plant, to allow for performance comparison between the two systems. The analysis aims to address three important topics related to FPV, particularly for this new technology. Firstly, this study reports on the performance and reliability over a one-year period.

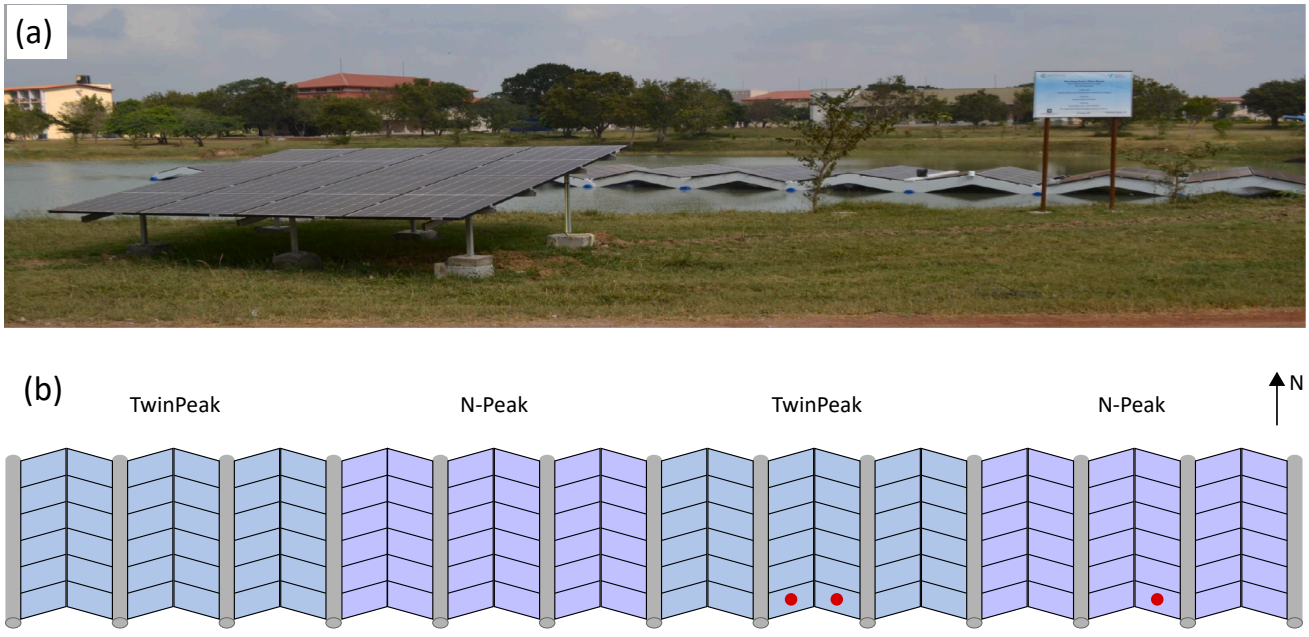


**Fig. 1.** (a) FPV system and GPV reference system (Current Solar AS, authorized). (b) Illustration of the FPV system with the location of the back panel temperature sensors marked with red dots. (For interpretation of the references to colour in this figure legend, the reader is referred to the web version of this article.)

**Table 1**
Summary of design features of the FPV and reference systems.

| System | Structure | Modules | Tilt & Orientation | System size (kW) |
|---|---|---|---|---|
| FPV system | Small footprint and relatively open structure. Air flow partially blocked by floating structure and surrounding panels. Direct exposure of the backside of the PV panels to the water surface. HDPE pipes provide the buoyancy to the system and the PV panels are mounted on composite beams. | REC Solar N-Peak 315 W and REC Solar TwinPeak 295 W | 15°, East-West | 44 |
| GPV system | Open Rack mounting structure installed on top of grass, enabling free flow of air in the back side of the PV modules. | REC Solar N-Peak 315 W | 8°, South | 2.5 |

The yield and performance ratio are calculated and compared to the GPV system. Secondly, thermal loss coefficients have been calculated based on production and weather data and have been implemented in PVsyst® to estimate the energy production of the FPV technology and benchmark it against measured data. Thirdly, as the FPV system in this study has been subject to a drought, leaving the installation sitting on a dry lakebed, the performance has been monitored before, during and after the drought.

This paper is organized as follows: Section 2 describes the system and the methodology used for performance assessments. The results are presented and discussed in Section 3, and a conclusion is given in Section 4.

## 2. Methodology

### 2.1. Case study description

The FPV system is installed in a freshwater body in Kilinochchi, in the province of Jaffna in Sri Lanka, with a GPV system installed in close vicinity. The studied FPV system is the first pilot from the company Current Solar AS, and both systems have been operating since January 2020. In the analysis data from March 2020 to May 2021 has been used. The system is situated at a latitude of 9.68 and longitude of 80.02. The local climate is characterized as a tropical rainforest, with warm temperatures and high humidity all year around. The yearly irradiation for a typical meteorological year (TMY), based on meteorological data from the Meteonorm database, is 1887 kWh/m$^2$ and the average temperature is 28.6 °C (World Bank Group, n.d.). The hottest and most humid months are April/May and August/September, respectively on each side of the monsoon rains, while the coolest months are December and January. This region is dominated by the North-eastern Monsoon, bringing the peak of rainfall to the region between the months October to December.

The studied FPV system has a rated installed capacity of 44 kW. The system consists of composite beams, where the solar panels are mounted, and high-density polyethylene (HDPE) pipes that provide buoyancy to the system. The composite beams are arranged in east–west orientation with a 15° tilt and the solar panels are mounted in portrait mode for maximum utilization of the standard-length HDPE pipe. Four of the strings are west facing, while the other four are east facing. The system is set up with two different module types, REC Solar N-Peak 315 W and REC Solar TwinPeak 295 W. The N-Peak modules are framed, monocrystalline n-type Si, and the Solar TwinPeak modules are framed, multi-crystalline Si modules. Each string contains 18 modules, and for each module type there are two strings facing west and two strings facing east, giving a total of eight strings in the FPV system. Each pair of strings with the same module type and orientation is connected in parallel to a separate maximum power point tracker (MPPT) on the same inverter. The FPV system has a relatively open structure, fitting into the "small footprint" classification suggested by Liu et al. (2018). The PV panels are mounted relatively close to the water surface, which will to some extent limit the air flow beneath the FPV system, see Fig. 1 a). The system is connected to a 50 kW SMA inverter with a total of 6 MPPTs.

The plant is instrumented with three Kipp&Zonen RT1 irradiance sensors, providing irradiance and back panel temperature, a Campbell Scientific 109 temperature sensor measuring water temperature ($T_w$), and a Campbell scientific CS215 air temperature and relative humidity sensor. Note that one of the irradiance sensors is defective. Data is logged with a Campbell Scientific CR310 datalogger. Fig. 1 b) shows the placement of the back panel temperature sensors.

A GPV reference plant with a rated capacity of 2.5 kW, is installed in close proximity to the FPV system, see Fig. 1 a). The GPV system consists of eight south facing REC Solar N-Peak 315 W type modules with an 8° tilt. In this study, only the strings consisting of the module type REC Solar N-Peak 315 W are assessed. The floating unit is instrumented with three POA irradiance sensors and module temperature ($T_m$) sensors, air temperature ($T_a$) and water temperature ($T_w$) sensors in addition to humidity. This instrumentation enables precise monitoring and performance analysis. The GPV system is connected to the same inverter as the FPV system, utilizing a separate MPPT. A summary of the design features for both the FPV and the reference system is given in Table 1.

**Table 2**
Summary of the filters and time periods used in the analysis.

| Topic | Metric | Data filtering | Time period |
|---|---|---|---|
| Overall FPV system performance | Temperature corrected performance ratio | Removal of: Times with missing irradiance data Irradiance = 0 | March 2020 – May 2021 |
| FPV vs GPV performance | Yield comparison, current and voltage comparison | Removal of: Morning and afternoon Shading ($\Delta P > 20\%$) | March 2020 - May 2021 |
| Heat loss coefficient | Eq. (5) | 6 h around solar noon Clear sky periods (Holmgren et al., 2018) | Jan 2021 - May 2021 |

### 2.2. Performance assessment

Different parameters for assessing the performance of PV systems are described in IEC 61724-1 (IEC, 2021). In this work, the performance ratio and relative yield is used to assess the overall performance of the system and compare the FPV and GPV system, respectively. Additionally, the heat loss coefficient is calculated using the Faiman model (Faiman, 2008). These different analyses will be explained in the following sections, with Table 2 listing the filters and given time period used for each.

#### 2.2.1. Performance ratios for the FPV system

The overall performance of the system is assessed through the performance ratio (PR), given by.

$$PR = \frac{\sum_t E_t / P_{STC}}{\sum_t H_{i,t} / G_{STC}} \quad (2)$$

where $E_t$ (kWh) is the energy output of the array at the given time, $P_{STC}$ (kW) is the nominal power (at standard test conditions, STC), $H_{i,t}$ (W/m$^2$) is the incident irradiation at the given time, and $G_{STC} = 1000$ W/m$^2$. It should be noted that $E_t$ constitutes the direct current (DC) energy of the east and west facing strings consisting of REC N-Peak 315 W modules. The temperature corrected performance ratio (CPR) is given by.

$$CPR = \frac{\sum_t E_t / P_{STC}}{\sum_t H_{i,t} / G_{STC} \times [1 + \gamma(T_{mod} - T_{STC})]}, \quad (3)$$

where γ is the module temperature coefficient, $T_{mod}$ (°C) is the module temperature and $T_{STC}$ = 25 °C. Both PR and CPR are calculated from March 2020 to May 2021. Due to an initial issue with the west facing irradiance sensor, the PR and CPR have been calculated for only the east facing string prior to 9th of November 2020. This was corrected on the 9th of November 2020, and after this, both west facing and east facing strings are including in the performance calculations. For PR and CPR calculations, the only filtering done is removal of time periods where the irradiance data is missing or equal to zero.

#### 2.2.2. Relative yield

A comparison between the mean performance of the west and east facing string on the FPV system and the south facing string of the GPV system is made by comparing the relative yield given by.

$$Y_{rel} = \frac{P_{FPV}/P_{FPV,STC} - P_{GPV}/P_{GPV,STC}}{P_{GPV}/P_{GPV,STC}} \times 100, \quad (4)$$

where $P_{FPV}$ (W) is the total power produced by the two REC N-Peak 315 W strings in the FPV system per day, $P_{GPV}$ (W) is the power produced by the ground system per day, and $P_{FPV,\ STC}$ (W) and $P_{GPV,\ STC}$ (W) are the nominal powers of the two systems respectively. To reduce the influence of instantaneous differences between the two systems, the daily yield is used. A yield comparison is chosen to compare the systems due to lacking POA irradiance measurements on the GPV system. For comparison of two systems with different orientation the relative yield is compared to the expected difference in available solar resource, based on clear sky modelling with pvlib (Holmgren et al., 2018). To ensure that effects of shading and individual system downtime are not taken into consideration when assessing the difference in yield, time periods where |Yrel| > 20% is removed, in addition to removal of morning (before 10:00) and afternoon values (after 16:00). The value of |Yrel| > 20% is set as a threshold as it was found to efficiently remove periods where one of the systems were down or shaded.

#### 2.2.3. Heat loss coefficient

In this work, the heat loss coefficient is calculated using.

$$U = \frac{G(\alpha - \eta(T_{mod}))}{T_{mod} - T_{amb}}, \quad (5)$$

where G (W/m$^2$) is the incident irradiance, α is the absorbed fraction of the incident irradiance, set to 0.9, $T_{mod}$ (K) is the module temperature, $T_{anb}$ (K) is the ambient temperature, and η is the power conversion efficiency of the module which is directly calculated from the produced power and measured incident irradiance.

Rapid changes in irradiance due to cloud movement may result in data points where the system is far from thermal equilibrium, resulting in incorrect estimates of the heat loss coefficient. To avoid this, only periods of clear sky are used for calculations of the heat loss coefficient. In addition, a filter is applied to select data only from a six-hour period around solar noon, to remove times during the morning and evening when the irradiance is changing more rapidly than during the middle of the day. After filtering approximately 5% of the data points with irradiance > 0 are left.

### 2.3. Output modelling

An energy yield analysis of the system using measured weather data was performed in PVsyst®, which is considered a standard for PV system design and simulation worldwide (Umar et al., 2018). It includes comprehensive meteorological and PV systems components databases. Irradiance and temperature data measured at the location from February to May 2021 was used as input data. Some days were missing from the measured irradiance data, in these cases the irradiance was assumed to be the same as the previous day. There were also some missing temperature measurements, which were filled in using logged weather forecasts from Yr ("Facts about Yr," n.d.). Currently, PVsyst® does not have an option to simulate FPV systems, but to some extent it is possible to adjust the available parameters to calculate the energy output of these systems. So, to calculate the energy yield for the FPV system, the calculated thermal loss coefficients, derived from temperature measurements, have been implemented into PVsyst® version 7.2.10. In the Faiman model implemented in PVsyst®, the parameters which may be altered are the constant thermal coefficient, $U_0$, the wind dependent thermal coefficient $U_1$, and the wind speed, $v$. The ambient air temperature and irradiance is by default imported from the selected meteorological data file. There is no direct way of including either the effect of water temperature or humidity in PVsyst®. However, the effect of water temperature for FPV systems that are not in direct contact with water is small: Lindholm et al. quantify the effects of water temperature and wind speed on the cell temperature for a FPV system with air-cooled rear side when the air temperature is kept constant (Lindholm et al., 2021). The results are shown in Table 3.

**Table 3**
Computed cell temperatures for different wind velocities and two water temperatures, 10 °C and 30 °C. The air temperature is kept constant at 30 °C.

| Wind [m/s] | $T_C$ [10 °C] | $T_C$ [30 °C] | $\Delta T_C$ |
|---|---|---|---|
| 1 | 52.75 | 56.47 | 3.72 |
| 3 | 46.20 | 48.92 | 2.72 |
| 5 | 42.49 | 44.58 | 2.09 |
| 7 | 40.23 | 41.91 | 1.68 |

Large variations in water temperature are required to significantly affect the cell temperature. Therefore, we can assume that the ambient air temperature, measured directly above the lake, is sufficient to provide an accurate representation of the thermal behaviour of the system. As reliable wind measurements were not available for the entire time period, a single U-value without a wind component is used.

In this study, a grid connected PV system is designed with the support of the mandatory input parameters of the software, including, but not limited to site location, local weather data, system components (inverters, modules), orientation and tilt of the PV modules, system sizing and detailed losses. The most relevant computation simulation parameters will be discussed below.

The light induced degradation (LID) loss is set to zero, as this is not a loss mechanism for n-type modules (ur Rehman and Hong Lee, 2013). The dynamic nature of the movement of floating solar designs was considered, as uneven sunlight reaching modules on the same string can cause differences mainly in current across connected modules, resulting in "mismatch losses". Since the FPV pilot site is a small in-land freshwater body, it was assumed that the waves and the resulting wave-induced mismatch is negligible. The mismatch loss was therefore set to 1% which is also the PVsyst® default value. The albedo of water is very low, around 0.06 (NSIDC, 2020), and since no measurements were performed at the location this parameter was conservatively set to 0.05. No near shading was included in the simulation, as there are no surrounding structures/objects which draw visible shades on the FPV system. Another relevant loss mechanism is soiling, which affects the ability of a PV cell to absorb irradiation, due to the accumulation of dirt (e.g., dust or bird droppings) on the surface of the solar module. Since the literature provides little quantitative information related to soiling for FPV systems and no measurements were done at the site; soiling losses were assumed to be 3%.

## 3. Results and discussion

In this study production and weather data from the first year of operation for an FPV system developed by Current Solar has been

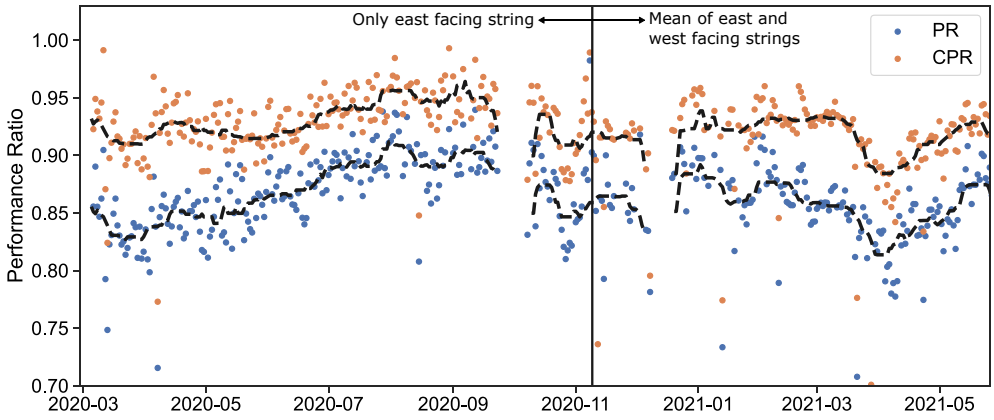


**Fig. 2.** Performance ratio (PR) and the temperature corrected performance ratio (CPR) for the N-Peak modules in the FPV system. The dotted lines are a rolling median. The vertical line marks when the issue with the west facing irradiance sensor was fixed. Points to the left of this line are calculated using only the east facing string, while points to the right are calculated using both east and west facing strings.

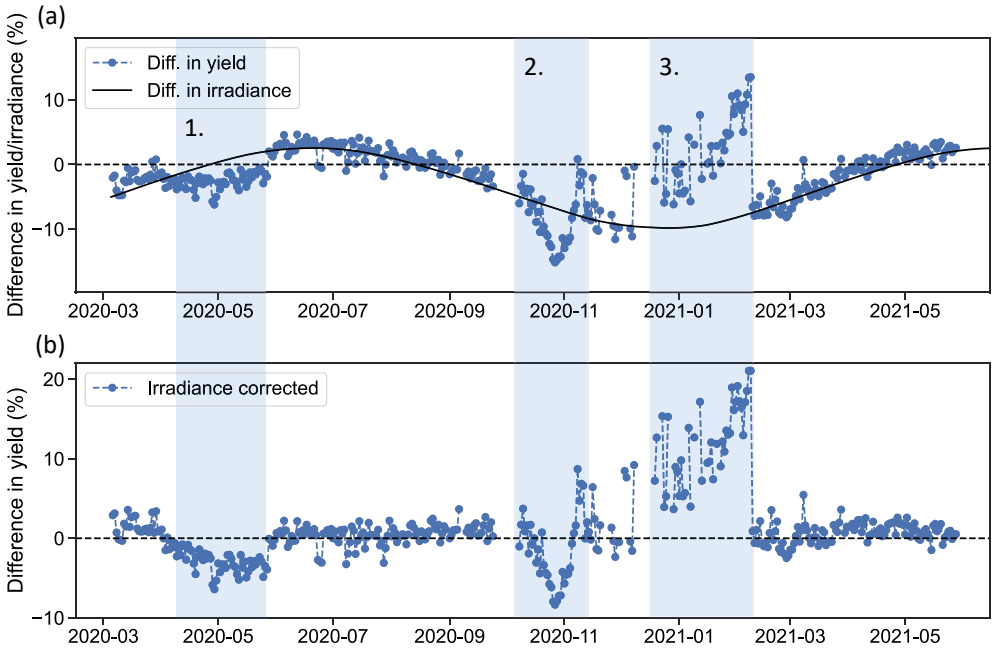


**Fig. 3.** Difference in yield of the floating system (averaged for east and west facing strings) and the ground mounted system. (a) shows values without correction for the difference in modelled irradiance due to different configurations, while this has been corrected for in (b).

analysed. In the following sections the results of the analysis are presented and discussed.

### 3.1. Performance and reliability

Fig. 2 shows the performance ratio (PR) (Eq. (2)) and the temperature corrected performance ratio (CPR) (Eq. (3)) aggregated to daily values in the period 6th of March 2020 to 26th of May 2021. Note that before 9th of November 2020 only PR for the east facing string is shown, see Section 2.2.1. The two periods of missing data are due to missing irradiance values.

Some of the variation in PR throughout the time period is corrected for by including the effect of temperature in CPR. However, some of the variation has other explanations, such as soiling and seasonal variation. An example of a possible seasonal variation is the observed reduction in CPR in the month of April, which can be seen in both years, but a longer period of data acquisition is needed to identify the seasonal variations and is outside the scope of this paper. The mean PR for the system in its first year of operation is 0.85, which is comparable with the four best performing systems at the FPV testbed in Singapore (Liu et al., 2018) Although more case studies and longer study periods are needed to establish a proper understanding of reliability, the observed stable PR over the studied period is a good first indication of a reliable technology.

The difference in yield, $Y_{rel}$, between the GPV and FPV system is shown in Fig. 3 a). An illustration of the expected difference in available solar resource due to the different system configurations, based on clear sky modelling (Holmgren et al., 2018), is included as a solid black line in Fig. 3 a). In Fig. 3 b) the modelled difference in available solar resource is subtracted from the relative yield. For times with a positive difference in yield, the FPV system is performing better compared to the GPV system and vice versa. In Fig. 3 a) and b), three time periods during the lifetime of the system are indicated as shaded areas 1, 2 and 3, and will be discussed in the following. In the first time period, the FPV system is underperforming for unknown reasons. The second period shows a clear drop in relative yield for the FPV system. In this time period the FPV system was no longer situated on water due to a period of drought. This will be discussed further in Section 3.3. In the third period, the FPV is performing better compared to the GPV system. During this time, there

are some large variations in the voltage levels of the GPV system, either due to a fault in the maximum power tracker or module faults. Apart from these three time periods, the average difference in yield is 0.6% in favour of the FPV system. This is within the margin of error of installed capacity and significance is therefore uncertain. The construction of the GPV system is more free standing than the FPV system, likely providing a higher cooling due to wind. Initial CFD calculations have shown that the wind cooling is expected to vary across the FPV system, depending on the wind direction, giving a temperature gradient across the FPV system, hence resulting in even higher difference in cooling by wind between the GPV and FPV system. While the GPV system is likely to have a higher wind cooling contribution, the FPV system is expected to have a slightly higher cooling contribution from thermal radiation between the module back cover and water (Lindholm et al., 2021).

### 3.2. Heat loss coefficients

For ground-mounted, freestanding systems a U-value of 29 W/m$^2$K is commonly used and is set as a default value in the performance assessment tool PVsyst® (PVsyst, n.d., n.d.). For fully insulated systems and intermediate cases, PVsyst® proposed U-values of 15 W/m$^2$K and 20 W/m$^2$K, respectively. However, the U-value is system specific, as shown by the broad range of values reported in the literature. Assuming a wind-speed of 1 m/s some examples of reported U-values for freestanding, ground-mounted systems are 18.5–28.5 W/m$^2$K (Ghabuzyan et al., 2021), 31.9 W/m$^2$K (Faiman, 2008) and 33–35.8 W/m$^2$K (Koehl et al., 2011). One study calculated U-values for freestanding systems in different climates with the same mounting and found a spread in U-values from 34.9 W/m$^2$K to 45.8 W/m$^2$K, assuming a wind speed of 1 m/s (Barykina and Hammer, 2017).

Fig. 4 shows heat loss coefficients (U-values) for the studied FPV system, calculated by inserting measured meteorological data in Eq. (5). A spread in U-values is observed, with a median of 32.6 W/m$^2$K and 32.5 W/m$^2$K for west and east facing strings respectively. For the west facing strings the 25th percentile is 30.9 W/m$^2$K and the 75th percentile is 38.0 W/m$^2$K. For the east facing strings the 25th percentile is 30.7 W/m$^2$K and the 75th percentile is 38.4 W/m$^2$K. The spread in values is likely due to the dependence of wind, which is not included in this study due to lack of reliable wind measurements. For FPV systems only a few previous studies have been undertaken. The heat loss coefficients derived for the Current Solar FPV system are lower than the experimentally determined median heat loss coefficients for a small footprint (U = 57 W/m$^2$K) system in the Netherlands, but similar to large footprint systems in the Netherlands (U = 37 W/m$^2$K) (Dörenkämper et al., 2021) and Singapore (U ~ 30 W/m$^2$K) (Liu et al., 2018).

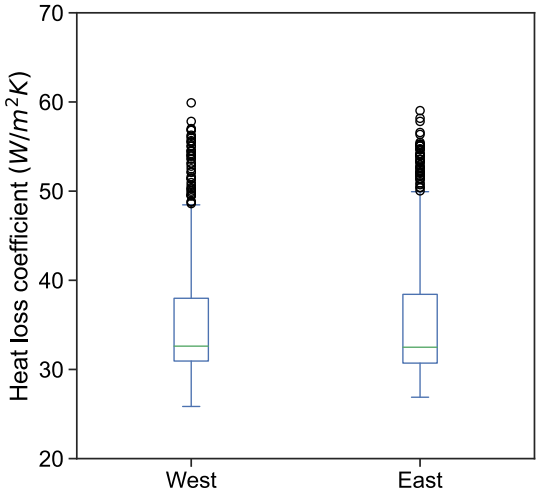


**Fig. 4.** Heat loss coefficient for the west and east facing string respectively, calculated from measured module temperatures and efficiency calculated from measured production and irradiation. The box spans the first to the third quartile, with the line indicating the median. The whiskers show the range of the data, and the points past the whiskers are outliers.

An energy yield analysis was done in PVsyst® with two different U-values, U = 33 W/m$^2$K and U = 20 W/m$^2$K, to see how the choice of U-value influences the expected PR and compare the results with measured data. Fig. 5 shows the resulting monthly PR values calculated from the measured data and the PVsyst® analysis. A U-value of 33 W/m$^2$K was chosen based on the median U-value found for this system. A U-value of 20 W/m$^2$K was chosen based on the default PVsyst® value for intermediate structures, since the structure of the FPV system limits wind cooling on the back side of the modules to some extent. A U-value of 33 W/m$^2$K provides the best fit to the measured data in February and May. In March and April, however, the PVsyst® model with a U-value of 20 W/m$^2$K provides a PR value that is closer to the measured performance. This may reflect an increase in module temperature due to reduced wind, or it may reflect other losses, not connected with operating temperature, that is currently not captured in the PVsyst® model. In March there is an increase in the difference between the module temperature and the air temperature, as seen in Fig. 6. This could be part of the reason why the measured PR decreases more than the PVsyst® PR from February to March, but the increase in temperature difference is not large enough to be the only contributing factor. Additionally, the temperature difference in April is similar to the difference in February and cannot explain the larger difference in PR in this month. It is therefore likely that the decrease in PR in March and April is due to other losses that are not captured in the PVsyst® model.

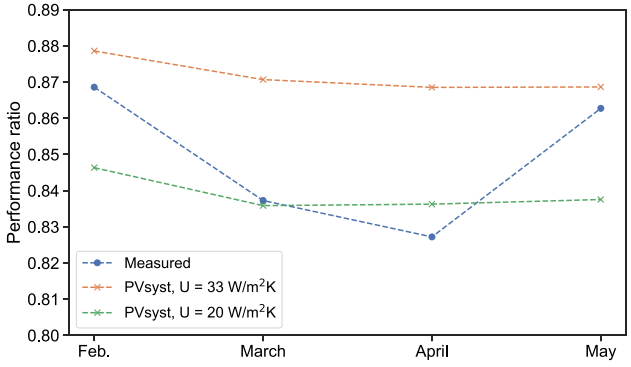


**Fig. 5.** Monthly performance ratio (PR) calculated from measured data compared to PR from an energy yield analysis in PVsyst® using measured weather data and two different U-values, U = 33 W/m$^2$K and U = 20 W/m$^2$K.

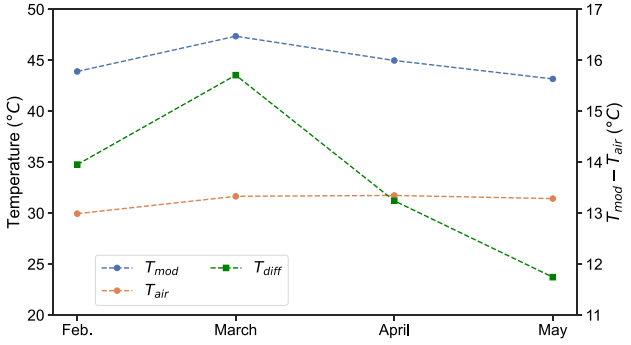


**Fig. 6.** Irradiance weighted module ($T_{mod}$) and air temperatures ($T_{air}$) aggregated to monthly values on the left axis. Difference between the irradiance weighted, monthly module and air temperatures ($T_{diff}$) on the right axis.

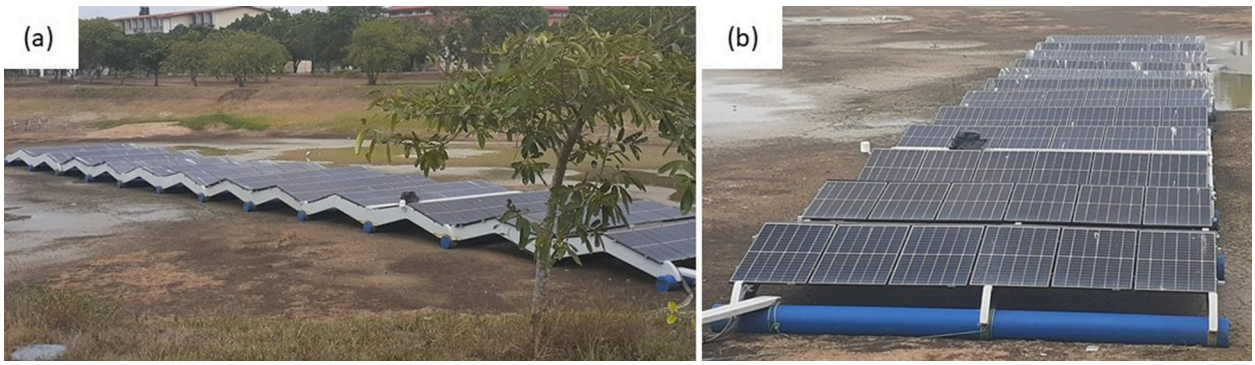


**Fig. 7.** (Current Solar AS, by permission) Picture of the FPV system in the months October and November 2020, when the system was located on the dry lakebed due to a period of drought.

### 3.3. *Effect of stranded FPV system dry bed*

Due to a period of drought, the lake where the FPV system is situated dried out in the months October and November 2020, as shown in Fig. 7. As shown in Fig. 3, the FPV system had a lower yield in this period compared to the GPV system. One hypothesis for the lower performance is that the lack of water leads to reduced water cooling. Such an effect would however result in lowered voltage levels, as the parameter predominantly affected by temperature variations is the voltage. Fig. 8 a) and b) shows the relative difference between the current and voltage levels of the FPV and GPV system. As the two systems have a different configuration, a normalization of the values has been done: 1) the current values of the FPV system are divided by four, as four strings in the FPV system are being compared to one string in the GPV system, 2) the voltage values of the FPV system are divided by 4.5, as two strings, each with two times 18 modules connected in parallel in the FPV system are being compared to one string with 8 modules in series in the GPV system. The relative difference for each data point is calculated and the result is aggregated to a daily median. Negative values imply lower values for the FPV system. We observe that the reduced performance is due to a drop in current levels and not in voltage for the FPV system. Hence, the drop in performance is most likely not due to a lack of cooling but could rather be caused by increased soiling on the FPV system, (as was observed in the picture shown in Fig. 7 b)), which becomes more evident in dry periods as the soiling is not washed away.

Comparing the relative yield difference between the FPV system and the GPV system (Fig. 3) in the months prior to the drought and after the dam is filled with water again, there is not significant change in the relative performance of the system. In a three-month period before the dry period the mean difference in yield was 0.4%, and in a three-month period after the dry period the difference in yield was 0.9%. This difference is smaller than the uncertainties related to seasonal variation and soiling. Additionally, Fig. 2 shows a decrease in CPR in October and November 2020, with the CPR values returning to pre-drought levels after the dam is filled with water again. The mean CPR in a three-month period before and after the drought is 0.92 and 0.91, respectively. Thus, the data indicate that the FPV system was unaffected by the drying of the lake. This means that amphibious systems can be a possibility, which is relevant for potential FPV sites where droughts can happen, or for installing FPV systems on new hydropower dams. However, this will be technology specific and further research is needed.

## 4. Conclusion

In this work we have studied the performance, reliability, and operational characteristics of a new FPV technology developed by Current Solar AS. The FPV system is located on a water body in Kilinochchi, Sri Lanka, with a ground-mounted PV system close by. Data from the first year of operation was collected and analysed, from which we can conclude.

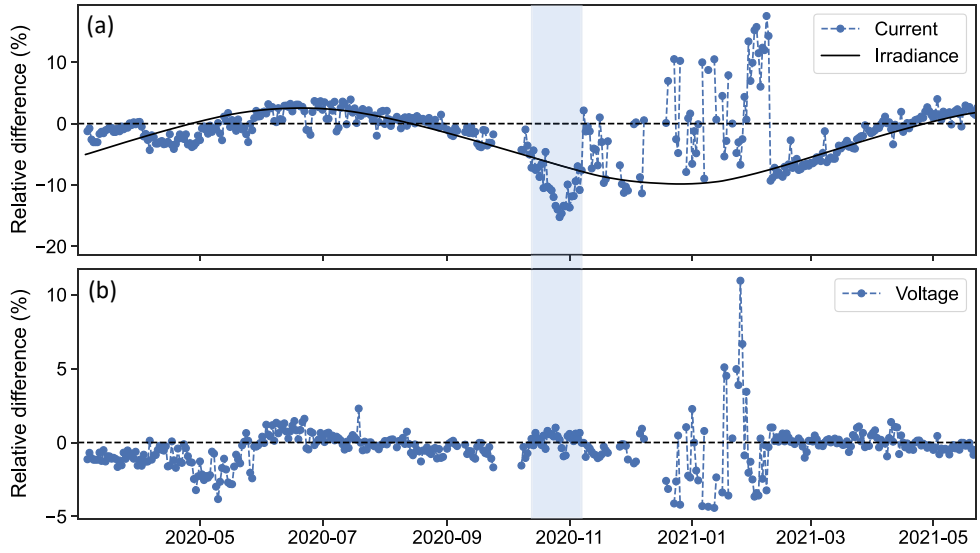


**Fig. 8.** Relative difference in normalized current (a) and voltage (b) between the FPV and the GPV system. The relative difference is calculated for each data point and then aggregated to a daily median.

- Analysis of the production data shows CPR values in the range of 0.9 and 0.95 after one year of operation.
- When compared with the closely situated GPV system, the relative yield difference during times of stable performance is 0.6% in favour of the FPV system, which is within the margin of error of installed capacity and is not considered a substantial difference in performance.
- The heat loss coefficient for the FPV system was calculated from temperature measurements, and a spread in U-values with a median of 33 W/m$^2$K, 25th percentile of 31 W/m$^2$K and 75th percentile of 38 W/m$^2$K was found.
- Although the dam where the FPV system is situated was dry for some period, we observe no implications for the continued performance of the system after the dam is yet again filled with water.

The results show an overall performance of the system in the same range as other FPV systems located in similar climates. Amphibious operation of the system does not affect the continued performance. To assess the degradation and reliability of the system, three years of operational data is needed and will be reported on a later stage.

## Declaration of Competing Interest

The authors declare that they have no known competing financial interests or personal relationships that could have appeared to influence the work reported in this paper.

## Acknowledgements

This work was supported by the Norwegian Research Council through project 309820. We would like to thank Equinor and Torgeir Ulset from Current Solar for facilitating the project and sharing the production data.

## References

Amiot, B., Chiodetti, M., le Berre, R., Radouane, K., Boublib, D., Patrick, D., Vermeyen, K., Giroux-Julien, S., 2020. Floating Photovoltaics – On-Site Measurements in Temperate Climate and Lake Influence on Module Behavior. In: 37th European Photovoltaic Solar Energy Conference and Exhibition. WIP, pp. 1772–1776. https://doi.org/10.4229/EUPVSEC20202020-6DO.15.2.

Barykina, E., Hammer, A., 2017. Modeling of photovoltaic module temperature using Faiman model: Sensitivity analysis for different climates. Sol. Energy 146, 401–416. https://doi.org/10.1016/j.solener.2017.03.002.

Cagle, A.E., Armstrong, A., Exley, G., Grodsky, S.M., Macknick, J., Sherwin, J., Hernandez, R.R., 2020. The Land Sparing, Water Surface Use Efficiency, and Water Surface Transformation of Floating Photovoltaic Solar Energy Installations. Sustainability 12, 8154. https://doi.org/10.3390/su12198154.

Cazzaniga, R., Cicu, M., Rosa-Clot, M., Rosa-Clot, P., Tina, G.M., Ventura, C., 2018. Floating photovoltaic plants: Performance analysis and design solutions. Renew. Sustain. Energy Rev. 81, 1730–1741.

Choi, Y.K., 2014. A study on power generation analysis of floating PV system considering environmental impact. Int. J. Software Eng. Appl. 8, 75–84. https://doi.org/10.14257/ijseia.2014.8.1.07.

Cox, M., 2019. The State of Floating Solar: Bigger Projects, Climbing Capacity, New Markets [WWW Document]. URL https://www.greentechmedia.com/articles/read/the-state-of-floating-solar-bigger-projects-and-climbing-capacity (accessed 12.14.21).

DNV GL, 2021. Recommended Practice. Design, development and operation of floating solar photovoltaic systems.

do Sacramento, E.M., Carvalho, P.C.M., de Araújo, J.C., Riffel, D.B., da Cruz Corrêa, R. M., Neto, J.S.P., 2015. Scenarios for use of floating photovoltaic plants in Brazilian reservoirs. IET Renewable Power Generat. 9, 1019–1024. https://doi.org/10.1049/iet-rpg.2015.0120.

Dörenkämper, M., Wahed, A., Kumar, A., de Jong, M., Kroon, J., Reindl, T., 2021. The cooling effect of floating PV in two different climate zones: A comparison of field test data from the Netherlands and Singapore. Sol. Energy 214, 239–247. https://doi.org/10.1016/j.solener.2020.11.029.

Dwivedi, P., Sudhakar, K., Soni, A., Solomin, E., Kirpichnikova, I., 2020. Advanced cooling techniques of P.V. modules: A state of art. Case Stud. Thermal Eng. 21 https://doi.org/10.1016/j.csite.2020.100674.

Facts about Yr [WWW Document], n.d. URL https://hjelp.yr.no/hc/en-us/articles/206550539-Facts-about-Yr (accessed 2.22.22).

Faiman, D., 2008. Assessing the outdoor operating temperature of photovoltaic modules. Prog. Photovoltaics Res. Appl. 16, 307–315. https://doi.org/10.1002/pip.813.

Folkerts, W., van Sark, W., de Keizer, C., van Hooff, W., van den Donker, M., 2017. ROADMAP PV Systemen en Toepassingen.

Gadzanku, S., Mirletz, H., Lee, N., Daw, J., Warren, A., 2021. Benefits and critical knowledge gaps in determining the role of floating photovoltaics in the energy-water-food nexus. Sustainability 13, 4317. https://doi.org/10.3390/su13084317.

Ghabuzyan, L., Pan, K., Fatahi, A., Kuo, J., Baldus-Jeursen, C., 2021. Thermal effects on photovoltaic array performance: Experimentation, modeling, and simulation. Appl. Sci. 11, 1460. https://doi.org/10.3390/app11041460.

Gorjian, S., Sharon, H., Ebadi, H., Kant, K., Scavo, F.B., Tina, G.M., 2021. Recent technical advancements, economics and environmental impacts of floating photovoltaic solar energy conversion systems. J. Cleaner Prod. 278, 124285 https://doi.org/10.1016/J.JCLEPRO.2020.124285.

Gross, G., 2017. Some effects of water bodies on the n environment-numerical experiments. J. Heat Island Inst. Int. 12.

Ho, C.J., Chou, W.L., Lai, C.M., 2016. Thermal and electrical performances of a water-surface floating PV integrated with double water-saturated MEPCM layers. Appl. Therm. Eng. 94, 122–132. https://doi.org/10.1016/j.applthermaleng.2015.10.097.

Holmgren, W.F., Hansen, C.W., Mikofski, M.A., 2018. pvlib python: a python package for modeling solar energy systems. Journal of Open Source Software 3, 884. https://doi.org/10.21105/joss.00884.

IEA, 2021. Global Energy Review 2021.

IEA, 2020. World Energy Outlook 2020.

IEC, 2021. Photovoltaic system performance - Part 1: Monitoring.

IEC, 2018. IEC 61853-2 Photovoltaic (PV) module performance testing and energy rating - Part 2: Spectral responsivity, incidence angle and module operating temperature measurements. Geneva.

IRENA, 2021. World Energy Transitions Outlook: 1.5°C Pathway.

Kamuyu, W.C.L., Lim, J.R., Won, C.S., Ahn, H.K., 2018. Prediction model of photovoltaic module temperature for power performance of floating PVs. Energies 11, 447. https://doi.org/10.3390/en11020447.

Kjeldstad, T., Lindholm, D., Marstein, E., Selj, J., 2021. Cooling of floating photovoltaics and the importance of water temperature. Sol. Energy 218, 544–551. https://doi.org/10.1016/j.solener.2021.03.022.

Koehl, M., Heck, M., Wiesmeier, S., Wirth, J., 2011. Modeling of the nominal operating cell temperature based on outdoor weathering. Sol. Energy Mater. Sol. Cells 95, 1638–1646. https://doi.org/10.1016/j.solmat.2011.01.020.

Kumar, M., Kumar, A., Gupta, R., 2021a. Comparative degradation analysis of different photovoltaic technologies on experimentally simulated water bodies and estimation of evaporation loss reduction. Prog. Photovoltaics Res. Appl. 29, 357–378. https://doi.org/10.1002/PIP.3370.

Kumar, M., Mohammed Niyaz, H., Gupta, R., 2021b. Challenges and opportunities towards the development of floating photovoltaic systems. Sol. Energy Mater. Sol. Cells 233, 111408. https://doi.org/10.1016/J.SOLMAT.2021.111408.

Lee, Y.G., Joo, H.J., Yoon, S.J., 2014. Design and installation of floating type photovoltaic energy generation system using FRP members. Sol. Energy 108, 13–27. https://doi.org/10.1016/j.solener.2014.06.033.

Lindholm, D., Kjeldstad, T., Selj, J., Marstein, E.S., Fjær, H.G., 2021. Heat loss coefficients computed for floating PV modules. Prog. Photovoltaics Res. Appl. 29, 1262–1273. https://doi.org/10.1002/PIP.3451.

Liu, H., Krishna, V., Lun Leung, J., Reindl, T., Zhao, L., 2018. Field experience and performance analysis of floating PV technologies in the tropics. Prog. Photovoltaics Res. Appl. 26, 957–967. https://doi.org/10.1002/pip.3039.

Liu, Luyao, Wang, Qinxing, Lin, Haiyang, Li, Hailong, Sun, Qie, Wennersten, Ronald, 2017. Power Generation Efficiency and Prospects of Floating Photovoltaic Systems. Energy Procedia 105, 1136–1142. https://doi.org/10.1016/j.egypro.2017.03.483.

Majid, Z.A.A., Ruslan, M.H., Sopian, K., Othman, M.Y., Azmi, M.S.M., 2014. Study on performance of 80 watt floating photovoltaic panel. J. Mech. Eng. Sci. 7, 1150–1156. https://doi.org/10.15282/jmes.7.2014.14.0112.

NSIDC, 2020. Thermodynamics: Albedo [WWW Document]. URL https://nsidc.org/cryosphere/seaice/processes/albedo.html (accessed 12.14.21).

Mittal, Divya, Saxena, Bharat Kumar, Rao, K.V.S., 2017. Comparison of Floating Photovoltaic Plant with Solar Photovoltaic Plant for Energy Generation at Jodhpur in India. In: IEEE International Conference on Technological Advancements in Power and Energy (TAP Energy ).

Oliveira-Pinto, S., Stokkermans, J., 2020. Marine floating solar plants: An overview of potential, challenges and feasibility. Proc. Inst. Civil Engineers - Maritime Eng. 173, 120–135. https://doi.org/10.1680/jmaen.2020.10.

Paton, C., 2021. Global Market Trends and Statistics of Floating Solar.

PVsyst, n.d. Project design > Array and system losses > Array Thermal losses [WWW Document]. URL https://www.pvsyst.com/help/thermal_loss.htm (accessed 12.20.21a).

PVsyst, n.d. Validations > Validations of old versions of the program [WWW Document]. URL https://www.pvsyst.com/help/validations_oldsystems.htm (accessed 12.20.21b).

Oliveira-Pinto, Sara, Stokkermans, Jasper, 2020. Assessment of the potential of different floating solar technologies – Overview and analysis of different case studies. Energy Convers. Manage. 211.

Rosa-Clot, M., Rosa-Clot, P., Tina, G.M., Scandura, P.F., 2010. Submerged photovoltaic solar panel: SP2. Renewable Energy 35, 1862–1865. https://doi.org/10.1016/J.RENENE.2009.10.023.

Skoplaki, E., Palyvos, J.A., 2009. Operating temperature of photovoltaic modules: A survey of pertinent correlations. Renewable Energy 34, 23–29. https://doi.org/10.1016/j.renene.2008.04.009.

Suh, J., Jang, Y., Choi, Y., 2020. Comparison of electric power output observed and estimated from floating photovoltaic systems: A case study on the Hapcheon dam, Korea. Sustainability 12, 276. https://doi.org/10.3390/su12010276.

Umar, N., Bora, B., Banerjee, C., Panwar, B.S., 2018. Comparison of different PV power simulation softwares: case study on performance analysis of 1 MW grid-connected PV solar power plant. Int. J. Eng. Sci. Invention 7, 11–24.

ur Rehman, A., Hong Lee, S., 2013. Advancements in n-Type Base Crystalline Silicon Solar Cells and Their Emergence in the Photovoltaic Industry. Scientific World J. 13 https://doi.org/10.1155/2013/470347.

Völker, S., Baumeister, H., Classen, T., Hornberg, C., Kistemann, T., 2013. Evidence for the temperature-mitigating capacity of urban blue space - A health geographic perspective. Erdkunde 67, 355–371. https://doi.org/10.3112/erdkunde.2013.04.05.

World Bank Group, n.d. Sri Lanka - Climatology | Climate Change Knowledge Portal [WWW Document]. URL https://climateknowledgeportal.worldbank.org/country/sri-lanka/climate-data-historical (accessed 12.14.21).

Yadav, N., Gupta, M., Sudhakar, K., 2017. Energy assessment of floating photovoltaic system, in: International Conference on Electrical Power and Energy Systems, ICEPES 2016. Institute of Electrical and Electronics Engineers Inc., pp. 264–269. https://doi.org/10.1109/ICEPES.2016.7915941.